Paramagnetic behaviour of silver nanoparticles generated by decomposition of silver oxalate

Hoa Le Trong [a, b, c], Kateryna Kiryukhina [a, d], Michel Gougeon [a, b], Valérie Baco-Carles [a, b], Frédéric Courtade [d], Sophie Dareys [d], Philippe Tailhades [a, b, *]

[a] Université de Toulouse, UPS, INPT, Institut Carnot Chimie Balard Cirimat, 118, route de Narbonne, F-31062 Toulouse Cedex 9, France
[b] CNRS, Institut Carnot Chimie Balard Cirimat, F-31062 Toulouse, France
[c] Ho Chi Minh City University of Science, Vietnam National University Ho Chi Minh City, 227 Nguyen Van Cu Q 5, 750000 Ho Chi Minh City, Viet Nam
[d] Centre National d'Etudes Spatiales, CNES, 18 Avenue Edouard Belin, 31 401 Toulouse Cedex 09, France

A B S T R A C T

Silver oxalate $Ag_2C_2O_4$, was already proposed for soldering applications, due to the formation when it is decomposed by a heat treatment, of highly sinterable silver nanoparticles. When slowly decomposed at low temperature (125 °C), the oxalate leads however to silver nanoparticles isolated from each other. As soon as these nanoparticles are formed, the magnetic susceptibility at room temperature increases from $-3.14\ 10^{-7}$ emu.Oe^{-1}.g^{-1} (silver oxalate) up to $-1.92\ 10^{-7}$ emu.Oe^{-1}.g^{-1} (metallic silver). At the end of the oxalate decomposition, the conventional diamagnetic behaviour of bulk silver, is observed from room temperature to 80 K. A diamagnetic-paramagnetic transition is however revealed below 80 K leading at 2 K, to silver nanoparticles with a positive magnetic susceptibility. This original behaviour, compared to the one of bulk silver, can be ascribed to the nanometric size of the metallic particles.

Keywords:
Silver oxalate
Silver nanoparticles
Paramagnetic silver
Oxalate decomposition
Nanocrystalline metal
Soldering

1. Introduction

1.1. Magnetic properties of noble metals nanoparticles

Bulk copper, silver or gold, display diamagnetic properties. Nanoparticles of such metals capped by surfactants or embedded in inorganic matrices, can however be paramagnetic or ferromagnetic [1–3]. Gold nanoparticles can exhibit paramagnetism. That was, for instance, observed when they are dispersed in poly-N-vinyl-2-pyrrolidone [4]. Gold nanoparticles functionalized by various ligands can also be ferromagnetic [5–8]. X-ray magnetic dichroïsm (XMCD) [9], muon spin relaxation [10] and ^{197}Au Mössbauer spectroscopy [2] have proved the direct contribution of gold to ferromagnetism. XMCD has also demonstrated the ferromagnetic contribution of copper and silver in thiol-capped nanoparticles [2]. Their saturation magnetization could be related to the strength of metal-ligand binding [11] even if that is still open to debate [12]. Ferromagnetism of uncapped gold or silver nanoparticles was however observed at room temperature [13,14] and theoretical studies have predicted ferromagnetism for clusters of bare noble metals [15–17]. In this work, paramagnetic properties are experimentally observed for the first time, in bare nanoparticles of silver resulting from the controlled thermal decomposition of silver oxalate.

1.2. Metals nanoparticles for low temperature soldering

From a technological point of view, metallic nanoparticles present a growing interest for low temperature soldering applications. Indeed, gallium nitride based electronic chips are increasingly used in power electronic systems. For space applications, their high power density makes the thermal management critical and requires thermal investigations. Usually, they are mounted to a thermal substrate by soldering and wiring bonding steps. The soldering process has to be carried out at moderate temperatures (<300 °C) and low contact pressures, to avoid irreversible damages or accelerated ageing effects on electronic devices. One of the thermal challenge is consequently to replace solder (as AuSn alloy) with a new material with intrinsic higher thermal conductivity and

* Corresponding author. Université de Toulouse, UPS, INPT, Institut Carnot Chimie Balard Cirimat, 118, route de Narbonne, F-31062 Toulouse Cedex 9, France.
E-mail address: tailhade@chimie.ups-tlse.fr (P. Tailhades).

http://dx.doi.org/10.1016/j.solidstatesciences.2017.05.009

which can be applied at moderate temperature. One way is to take benefit of the strong lowering of melting temperature alloys when the particle size of such metals is strongly reduced below 10 nm [18–20]. Because the sintering generally occurs at an absolute temperature close to 80% of the melting point, this decrease makes low-temperature sintering easier.

1.3. Specificities of silver oxalate

The silver oxalate ($Ag_2C_2O_4$) is an interesting compound for such mounting applications, because its decomposition, already described by taking into account the structural specificities [21,22], leads to silver nanoparticles according to the simple following reaction:

$$Ag_2C_2O_4 \rightarrow 2Ag + 2CO_2$$

The resulting nanoparticles have the required high sintering propensity in the range 200–300 °C and the metallic silver formed at the end of the soldering process has a high intrinsic thermal conductivity [23]. Moreover, the silver oxalate is easily decomposed as illustrated by Fig. 1, which shows the spherical nanoparticles of silver generated by a scanning electron microscope, at the end of several scans. The silver nanoparticles are arranged according to a regular lattice, which corresponds to the periodicity of the electron beam modulation. This periodicity is close to 76 nm for the images (b), (c) and (d) in Fig. 1. Silver oxalate also decomposes in air, in inert or reducing atmosphere, by heating it above 100 °C or by applying mechanical stresses. Additionally, because the decomposition of silver oxalate is highly exothermic, a proper heating procedure provides void mitigation in the solder joint. This joint having a high thermal conductivity, is obtained without heating the chip to solder, above 300 °C [24]. A very slow decomposition carried out in between 100 and 130 °C for several hours, allows also a complete decomposition. In that instance, isolated nanoparticles of silver are obtained by this way.

2. Materials and methods

The starting oxalate powder was prepared as follow. A concentrated solution of silver nitrate (2 mol l^{-1}) was reacted with oxalic acid solution (0.5 mol l^{-1}) to produce a precipitate of oxalate. The silver nitrate (purity > 99.9%) was initially dissolved in a mixture of deionised water (10% vol.) and analytical grade ethylene glycol (90% vol.). Oxalic acid was dissolved in a mixture of absolute ethyl alcohol (95% vol.) and deionised water (5% vol.). After precipitation, the oxalate was separated from the liquors by centrifugation and washed by deionised water. This operation was repeated five times. The oxalate was then dried at 50 °C.

The silver oxalate and metallic silver were characterised by X-ray diffraction with a Siemens D 5000 diffractometer equipped with a Brucker sol-X detector. The X-ray wavelength was that of the copper Kα ray (Kα1 = 0.15405 nm and Kα2 = 0.15443 nm). The chemical composition of the metallic powder was analysed by Inductively Coupled Plasma – Mass Spectroscopy (ICP-MS). The samples were also investigated by two scanning electron microscopes (SEM), a SEM ZEISS Ultra 55 and a field emission gun SEM JEOL JSM 6700 F equipped with an Energy-dispersive X-ray spectroscopy (EDS) system of Princeton Gamma Tech.

The magnetic properties were measured with a vibrating sample magnetometer (VSM Quantum Design Versalab) and a SQUID magnetometer MPMSXL 7 from Quantum design. The decomposition of the silver oxalate was carried out inside the VSM, which is equipped with a system of heating up to 400 K. For such

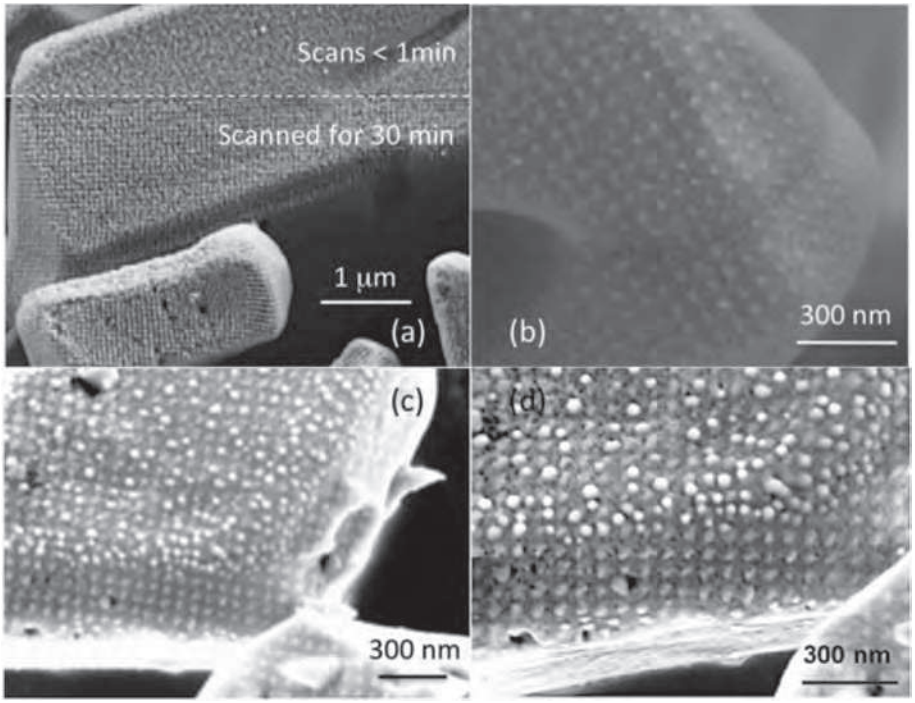

Fig. 1. Silver oxalate particles observed by scanning microscopy. (a): The lower part of the sample in image (a) was originally scanned for 30 min by a 300 pA and 3 kV electron beam. The scanned region was then enlarged and an image was recorded after a few additional scans lasting less than 1 min. The image obtained clearly shows two regions. At the bottom there is a texturing induced by the pulsed energy of the electron beam, which is responsible of the partial decomposition of the oxalate. This latter is not modified in the upper part of the image. (b) Image of freshly prepared silver oxalate after scans for 10 min at 200 nA and 3 kV. Silver particles are arranged according to a periodic network with a lattice constant of 76 nm, corresponding to the electron beam modulation. (c) Image after scans for 10 min at 200 nA and 3 kV, of a silver oxalate initially heated at 20 °C.min^{-1} up to 210 °C then quenched. (d) Detail of image c.

temperature measurements, the studied oxalate powders were placed in an aluminium sheet and a brass sample holder. The VSM was then used for the measurements at different steps of oxalate decomposition. Due to the limited operating temperatures of the apparatus, such measurements were done in a range lying from 50 to 300 K. Measurements at lower temperatures were performed with the SQUID, without removing the sample from its sample holder and taking the best precautions, to avoid possible contamination during transfer. The package composed of the aluminium container and the sample holder, was measured to have data of magnetization as a function of temperature, to perform baseline corrections.

3. Results and discussion

The powder obtained by the chemical precipitation previously described, is a $Ag_2C_2O_4$ pure silver oxalate, as revealed by X-ray diffraction pattern (Fig. 2). The mass loss after complete decomposition in air into metallic silver, is close to 28.97% in agreement with a decomposition of $Ag_2C_2O_4$ leading to metallic silver and CO_2 gas.

The beginning of silver oxalate decomposition is revealed by the metallic silver formation in Fig. 2 and illustrated by Fig. 3 showing the appearance of the silver nanoparticles at the surface of the initial oxalate particles. Partially decomposed oxalate particles displays a very porous microstructure as it can be observed on a particle section prepared by microtomy (Fig. 4). Silver nanometric particles are still blocked in the cavities, formed by the decomposition, and isolated from the other metallic grains. Their sintering is thus delayed up to the whole decomposition of the oxalate. Transmission electron microscopy is not possible to carry out because of the high sensitivity of the oxalate to a focused electron beam. Consequently, more details about the microstructure and the localisation of the metallic nanoparticles were not obtained.

The starting silver oxalate displays diamagnetic properties from 50 K (−223 °C) up to room temperature. After subtraction of the container and sample holder contributions, the silver oxalate susceptibility was derived. A value of $-3.14 \pm 0.02\ 0.10^{-7}$ emu.Oe^{-1}.g^{-1} at room temperature was obtained.

Measurements of the magnetization at 20 kOe, in the range of temperature lying from room temperature to 50 K (−223 °C), were also carried out at various states of progress of decomposition

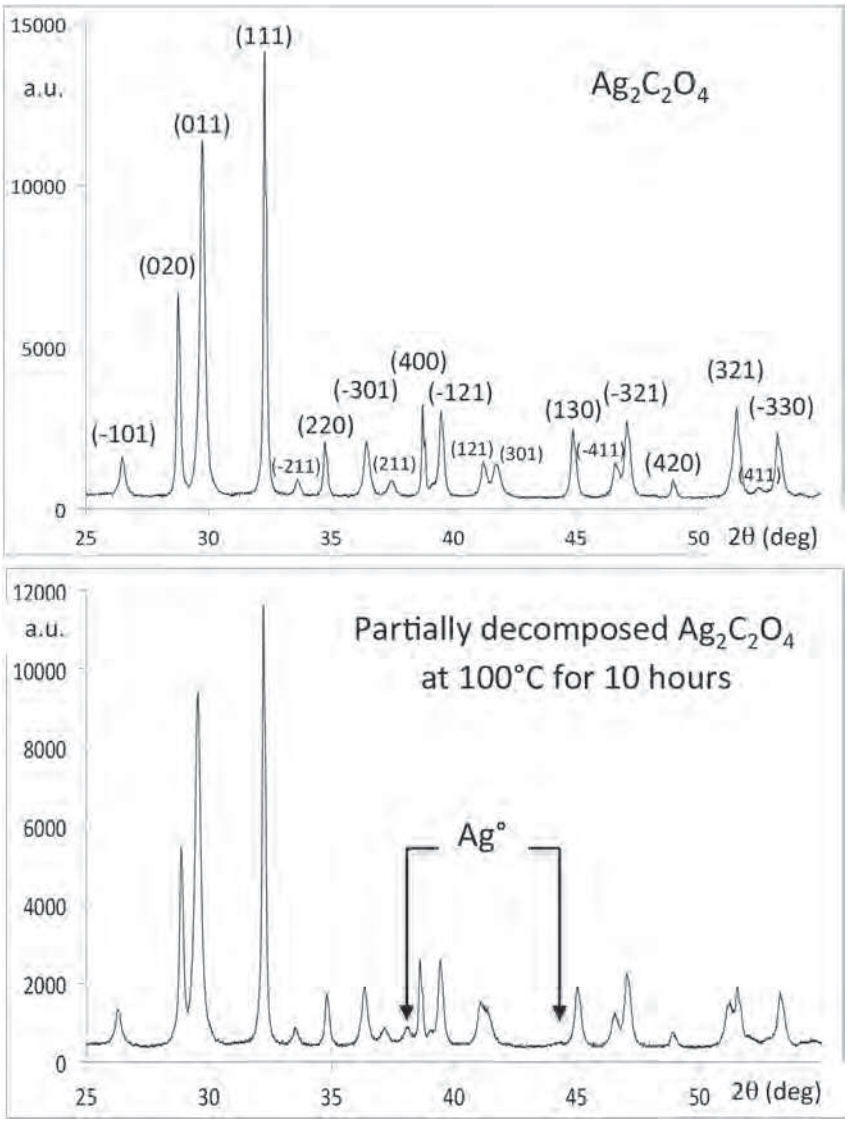

Fig. 2. X-ray diffraction patterns of pure silver oxalate and after its partial decomposition at 100 °C for 10 h.

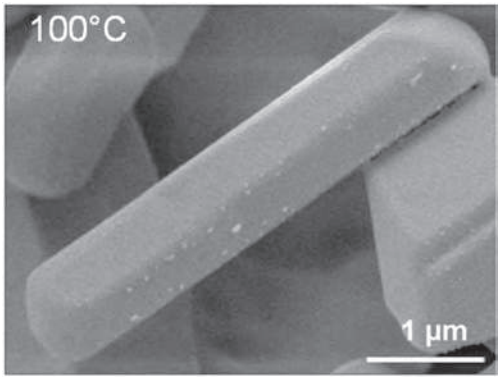

Fig. 3. Metallic silver nanoparticles (bright dots) growing at the surface of silver oxalate crystals. The oxalate was partially decomposed in air at 100 °C for 10 h.

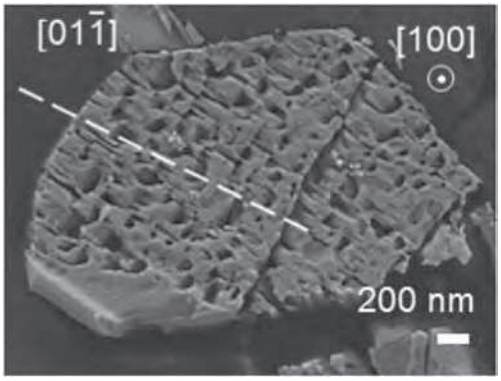

Fig. 4. Transversal section of a silver oxalate particle decomposed at 130 °C for 10 h. Some metallic silver nanoparticles (bright dots) can be observed inside the porosity generated by the oxalate decomposition. Two crystallographic axes for the oxalate particle are shown.

(Fig. 5). At 125 °C, the kinetic of formation of silver particles from an oxalate is slow. It is the reason why the processing times have been long enough. However, clear changes in the magnetization versus temperature curves, were observed after heat treatment (Fig. 5a). In the range of temperature above about 80 K (−193 °C), the diamagnetic behaviour still remains but the magnetic susceptibility increases progressively to reach $-1.90 \pm 0.02\ 0.10^{-7}$ emu.Oe^{-1}.g^{-1}, after 100 h of heat treatment. This value is calculated dividing the magnetization by the mass sample after treatment and by the applied field (20 k Oe). This susceptibility is very close to the one of pure bulk silver. In fact, bibliographical data give $-1.95.10^{-7}$ emu.Oe^{-1}.g^{-1} [24] and our measurements, carried out on a silver bulk sample obtained by oxalate decomposition in air at 900 °C, give $-1.92 \pm 0.02\ 0.10^{-7}$ emu.Oe^{-1}.g^{-1}. These results highlight the complete decomposition of the oxalate into metallic silver after a long term heat treatment at 125 °C. For such a sample, the magnetization is no more constant with temperature. The same behaviour is observed for the partially decomposed oxalate at 125 °C for only 10 h. It is interesting to plot the susceptibility per gram of metallic silver, versus temperature, for the totally (125 °C-100 h) and partially (125 °C-10 h) decomposed samples. For the partially decomposed sample, the metallic silver quantity was estimated from the reaction:

$$Ag_2C_2O_4 \rightarrow (1-x)\ Ag_2C_2O_4 + 2x\ Ag + 2x\ CO_2,$$

which shows that the solid part remaining after a treatment at 125°-10 h is (1-x) $Ag_2C_2O_4$ + 2x Ag. The ratio of the molar mass of these residual compounds multiplied by their molar fractions to the molar mass of the initial oxalate, is equal to the mass of the sample after treatment divided by the mass of the oxalate initially introduced into the magnetometer. In our case, this amounts to writing that:

$$(303.74 - 88x)/303,74 = 68.71.\ 10^{-3} \Big/ 74.78.\ 10^{-3}$$

with:

(303.74−2(44)x) = molar mass in grams of (1-x) $Ag_2C_2O_4$ + 2x Ag
303.74 g = molar mass in grams of silver oxalate, 44 g = molar mass of CO_2
$68.71.\ 10^{-3}$ = sample mass after a treatment at 125-10 h
$74.78.\ 10^{-3}$ = initial oxalate sample mass.
This gives x = 0.2802 or a mass of metallic silver equal to 14.87 mg resulting from the partial decomposition of the initial 74.78 mg of silver oxalate.

Fig. 5b shows also clearly the change in magnetic properties at low temperature for the two samples. It reveals also a stronger change in susceptibility for the partially decomposed sample.

The behaviour of the totally decomposed sample was studied at lower temperature with a SQUID magnetometer. Below 80 K, the magnetization exhibits a peak centred around 60 K (−213 °C) for zero field cooled (ZFC) curve and around 40 K for field cooled (FC) curve, followed, at the lowest temperatures, by a paramagnetic tail in each case (Fig. 6a). The plot of the magnetization versus field at 2 K confirms the paramagnetic-like behaviour of the decomposed oxalate (Fig. 6b).

The resulting product of decomposition at 125 °C for 100 h, was carefully analysed after the magnetic measurements. In agreement with the susceptibility measurements, it was made of metallic silver and the presence of oxalate was not detected. The silver was in the form of spherical nanoparticles with some truncations for the largest ones (Fig. 7). Their “diameters” lied from about 5 to 20 nm. Careful analyses by both Energy-dispersive X-ray spectroscopy (EDS) and Inductively Coupled Plasma − Mass spectroscopy (ICP-MS) allowed to determine their chemical composition. The particles contain more than 99.52 mass. % of silver. Conventional ferromagnetic metals such as iron, cobalt, nickel or gadolinium, have been tracked also, but their concentrations were less than 50 ppm. Transition metals were not detected at a concentration higher than 50 ppm. Less than 0.5 mass. % of carbon impurities were also detected. On the other hand, X-ray diffraction patterns didn't reveal any other phase than pure metallic silver.

The unconventional paramagnetic behaviour observed at low temperatures for the silver nanoparticles, cannot then be assigned to superparamagnetic impurities such as iron, cobalt, nickel or gadolinium metallic nanoparticles, because they are only present in trace amounts in the powder studied. Some authors have already assumed that carbon brings a small and soft ferromagnetic contribution in silver-carbon composites with 70 mass. % of carbon [25]. According to previous analysis, the concentration of this element is however much lower in the silver powder issued from oxalate and it gets obvious not to incriminate carbon impurities to be responsible for the paramagnetism observed. The paramagnetic behaviour observed at low temperature, seems therefore due to intrinsic properties of bare silver nanoparticles. These magnetic properties are unconventional for silver and they are even more original because silver is not capped by molecules, such as thiols, which generally change the magnetic properties of noble metal because of strong bonds with the metal and a resulting charge

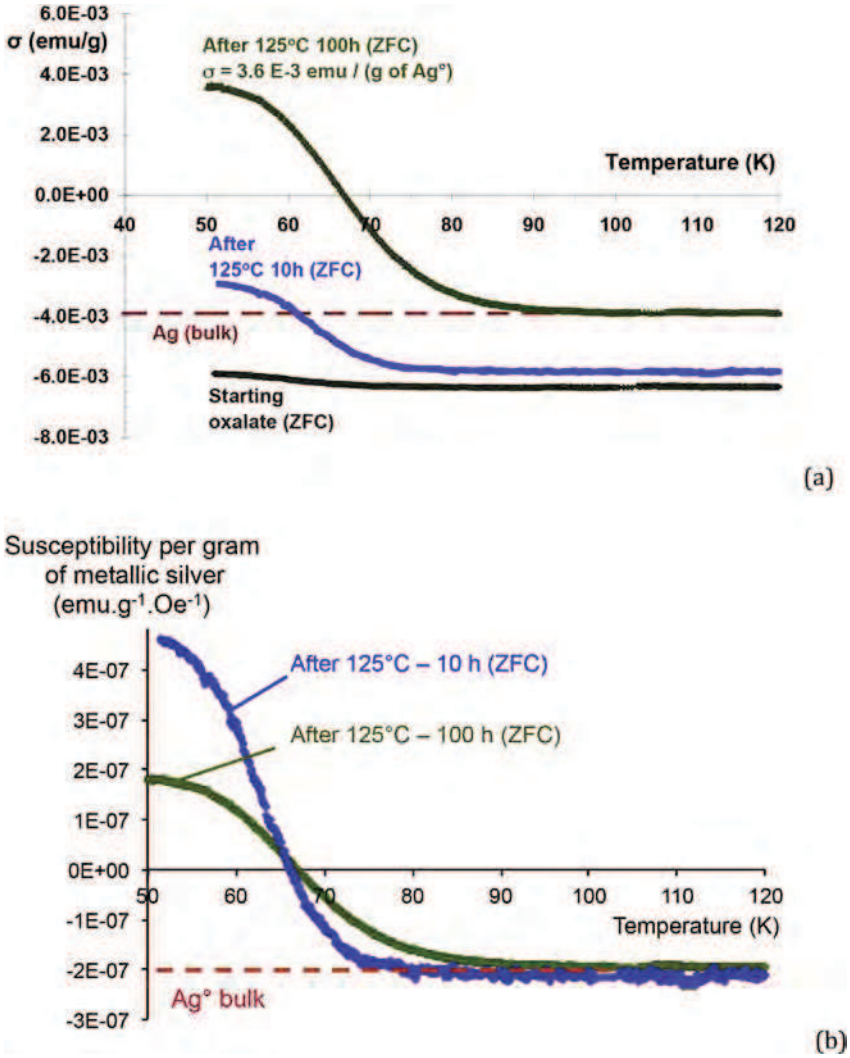

Fig. 5. (a) Zero field cooled magnetization under 20 kOe at different temperatures, for an oxalate sample at the early beginning of the decomposition, after 10 h and 100 h at 125 °C. The heat treatments were carried out inside the vibrating sample magnetometer to avoid contamination. The magnetization is divided by the sample mass measured after heat treatment. The magnetization under 20 kOe for diamagnetic bulk silver is given for comparison. (b) Susceptibility per gram of metallic silver formed after heat treatment, versus measurement temperature. The susceptibility of bulk silver is given for comparison.

transfer. Therefore, low temperature paramagnetism appears to be related to a size effect only. The logic of this interpretation is reinforced by the results presented in Fig. 5b. It shows a more marked change in magnetic behaviour per unit of silver mass formed for the partially decomposed sample. As can be illustrated in Figs. 3 and 4, this sample is precisely composed of silver particles still isolated in the oxalic matrix, which are smaller than after the total decomposition. The latter obviously generates a slight growth of the grains of metallic silver.

It is however difficult to go further in the interpretation of observed physical phenomena. The theory of the persistent currents [26], which gives an interpretation of the unusual magnetic properties of gold in the nanometric state, could bring elements of understanding to the diamagnetic-paramagnetic transition highlighted. However, caution should be exercised in the absence of further investigation.

The interest of the experimental protocol used in this article lies in the formation of nanoparticles within the magnetometer itself. This makes it possible to consider many experiments. In particular, it would be possible to form nanoparticles of slightly different sizes under different fields and to measure the effect on the paramagnetic properties at low temperature. The identification of a link between the intensity of these fields, the particle size and the paramagnetic behaviour, could then reinforce the interpretation based on the existence of persistent currents. The differences observed in Fig. 6a for the ZFC and FC samples may suggest a positive outcome for this type of measurements. It will be necessary to verify all this.

4. Conclusion

In conclusion, the interest in the silver oxalate is not reduced to its suitability for soldering of components for the space industry. It is also a very good precursor for fundamental scientific studies. Indeed, due to its quite low stability, silver oxalate can be totally decomposed at low temperature (125 °C) to obtain pure metallic silver nanoparticles. These latter are diamagnetic at room temperature but they have a paramagnetic-like behaviour below 80 K (−193 °C).

The pollution of the samples by impurities appears not suspected because of the experimental precautions setup. Moreover, the paramagnetic-diamagnetic transition at low temperature, is not common among the materials used to manipulate the samples or among the most common ferro or ferrimagnetic materials having a

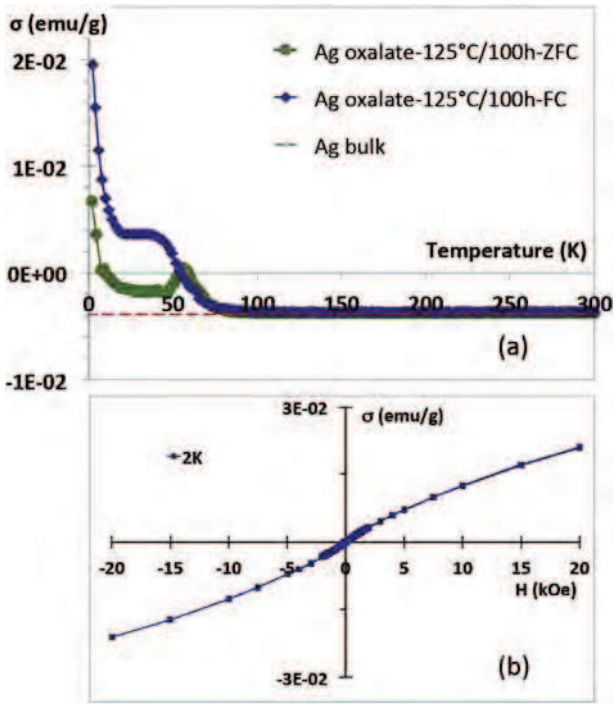

Fig. 6. (a) Magnetization per gram of metallic silver versus temperature. For temperature higher than about 80 K, the nanoparticles are diamagnetic as bulk silver. Below 80 K, a diamagnetic-paramagnetic transition occurs. (b) At 2 K the silver nanoparticles are clearly paramagnetic as it is highlighted by the magnetization versus field curve.

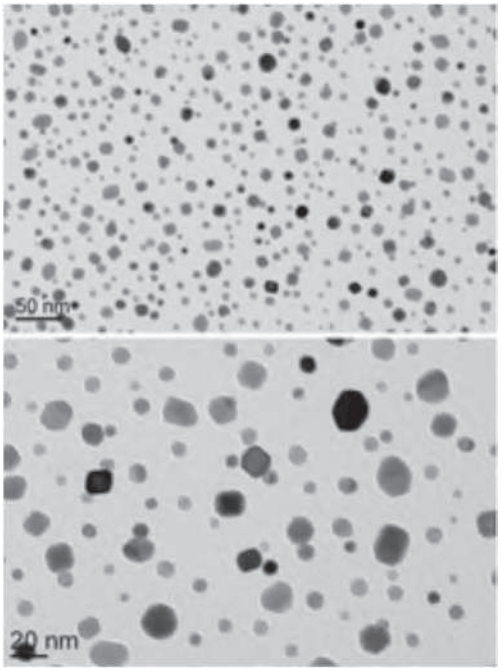

Fig. 7. Silver nanoparticles obtained after heat treatment of the silver oxalate at 125 °C for 100 h in helium atmosphere, inside the vibrating sample magnetometer used for the magnetic measurements. For both (a) and (b) images, the silver powder was previously dispersed in alcohol in an ultrasonic bath, before observation, to obtain well-separated particles.

high magnetic signal, such as iron alloys or iron oxides. Consequently, it seems that the magnetic properties observed are really related to metallic silver.

Appendix A. Supplementary data

Supplementary data related to this article can be found at http://dx.doi.org/10.1016/j.solidstatesciences.2017.05.009.

References

[1] L. Suber, F. Dino, G. Scavia, P. Imperatori, W.R. Plunkett, Permanent magnetism in dithiol-capped silver nanoparticles, Chem. Mater 19 (6) (2007) 1509–1517.
[2] J.S. Garitaonandia, M. Insausti, E. Goikolea, M. Suzuki, J.D. Cashion, N. Kawamura, H. Ohsawa, I. Gil de Muro, K. Suzuki, F. Plazaola, T. Rojo, Chemically induced permanent magnetism in Au, Ag and Cu nanoparticles: localization of the magnetism by element selective techniques, Nano. Lett. 8 (2) (2008) 661–667.
[3] S. Trudel, Unexpected magnetism in gold nanostructures: making gold even more attractive, Gold Bull. 44 (2011) 3–13.
[4] H. Hori, T. Teranishi, Y. Nakae, Y. Seino, M. Miyake, S. Yamada, Anomalous magnetic polarisation effect of Pd and Au nano-particles, Phys. Lett. A 263 (1999) 406–410.
[5] H. Hori, Y. Yamamoto, T. Iwamoto, T. Miura, T. Teranishi, M. Miyake, Diameter dependence of ferromagnetic spin moment in Au nanocrystals, Phys. Rev. B 69 (2004) 174411.
[6] P. Crespo, R. Litran, T.C. Rojas, M. Multigner, J.M. de la Fuente, J.C. Sanchez-Lopez, M.A. Garcia, A. Hernando, S. Penades, A. Fernandez, Phys. Rev. Lett. 93 (2004), 087204 and 94 (2005) 049903(E).
[7] M.A. Munoz-Marquez, E. Guerrero, A. Fernandez, P. Crespo, A. Hernando, R. Lucena, J.C. Conesa, Permanent magnetism, magnetic anisotropy, and hysteresis of thiol-capped gold nanoparticles, J. Nanopart. Res. 12 (2010) 1307–1318.
[8] B. Donnio, P. Garcia-Vazquez, J.-L. Gallani, D. Guillon, E. Terazzi, Dendronized ferromagnetic gold nanoparticles self-organized in a thermotropic cubic phase, Adv. Mater 19 (2007) 3534–3539.
[9] Y. Yamamoto, T. Miura, M. Suzuki, N. Kawamura, H. Miyagawa, T. Nakamura, K. Kobayashi, T. Teranishi, H. Hori, Direct observation of ferromagnetic spin polarization in gold nanoparticles, Phys. Rev. Lett. 93 (2004) 116801.
[10] E. Goikolea, J.S. Garitaonandia, M. Insausti, J. Lago, I. Gil de Muro, J. Salado, F.J. Bermejo, D. Schmool, Evidence of intrinsic ferromagnetic of thiol capped Au nanoparticles based on μSR results, J. Non-Cryst. Solids 354 (2008) 5210–5212.
[11] U. Maitra, B. Das, N. Kumar, A. Sundaresan, C.N.R. Rao, Ferromagnetism exhibited by nanoparticles of noble metals, ChemPhysChem 12 (2011) 2322–2327.
[12] G.L. Nealon, B. Donnio, R. Greget, J.-P. Kappler, E. Terazzi, J.-L. Gallani, Magnetism in gold nanoparticles, Nanoscale 4 (2012) 5244–5258.
[13] S. Mohapatra, R.K. Kumar, T.K. Maji, Green synthesis of catalytic and ferromagnetic gold nanoparticles, Chem. Phys. Lett. 508 (2011) 76–79.
[14] Y. Jo, M.H. Jung, M.C. Kyum, S.I. Lee, Ferromagnetism signal in nanosized Ag particles, J. Nanosci. Nanotechnol. 7 (11) (2007) 3884–3887.
[15] M. Pereiro, D. Baldomir, J.E. Arias, Unexpected magnetism of small silver clusters, Phys. Rev. A 75 (2007) 063204.
[16] F. Chen, R.L. Johnston, Charge transfer driven surface segregation of gold atoms in 13-atom Au-Ag nanoalloys and ots relevance to their structural, optical and electronic properties, Acta. Mater 56 (2008) 2374–2380.
[17] W. Li, F. Chen, A density functional theory study of structural, electronic, optical and magnetic properties of small Ag-Cu nanoalloys, J. Nanopart. Res. 15 (2013) 1809.
[18] Ph Buffat, J.P. Borel, Size effect on the melting temperature of gold particles, Phys.Rev. A 13 (6) (1976) 2287–2298.
[19] A.N. Goldstein, C.M. Echer, A.P. Alivisatos, Melting in semiconductors nanocrystals, Science 256 (5062) (1992) 1425–1427.
[20] A. Hu, J.Y. Guo, H. Alarifi, G. Patane, Y. Zhou, G. Compagnini, C.X. Xu, Low temperature sintering of Ag nanoparticles for flexible electronics packaging, Appl. Phys. Lett. 97 (153117) (2010) 1–3.
[21] D.Y. Naumov, E.V. Boldyreva, N.V. Podberezskaya, J.A.K. Howard, The role of "ideal" and "real" crystal structure in the solid-state decomposition of silver oxalate: experimental diffraction studies and theoretical calculations, Solid State Ionics 101–103 (1997) 1315–1320.
[22] V.V. Boldyrev, Thermochim.,Thermal decomposition of silver oxalate, Acta 388 (2002) 63–90.
[23] K. Kiryukhina, H. Le Trong, Ph Tailhades, J. Lacaze, V. Baco, M. Gougeon, F. Courtade, S. Dareys, O. Vendier, L. Raynaud, Silver oxalate-based solders: new materials for high thermal conductivity microjoining, Scr. Mater 68 (2013) 623–626.
[24] Landolt-Bornstein, Numerical Data and Functional Relationships in Science and Technology, New Series, II/16, Diamagnetic Susceptibility, Springer-Verlag, Heidelberg, 1986, pp. 4–134.
[25] R. Caudillo, X. Gao, R. Escudero, M. José-Yacaman, J.B. Goodenough, Ferromagnetic behaviour of carbon nanospheres encapsulating silver nanoparticles, Phys. Rev. B 74 (2006) 214418.
[26] R. Gréget, G.L. Nealon, B. Vileno, Ph Turek, Ch Mény, F. Ott, A. Derory, E. Voirin, E. Rivière, A. Rogalev, F. Wilhelm, L. Joly, W. Knafo, G. Ballon, E. Terazzi, J.P. Kappler, B. Donnio, J.L. Gallani, Magnetic properties of gold nanoparticles: room-temperature quantum effect, ChemPhysChem 13 (2012) 3092–3097.